IEEE Access
Multidisciplinary | Rapid Review | Open Access Journal

Received 2 April 2023, accepted 12 April 2023, date of publication 17 April 2023, date of current version 1 May 2023.

Digital Object Identifier 10.1109/ACCESS.2023.3267801

RESEARCH ARTICLE

Optimal Location and Sizing of Electric Bus Battery Swapping Station in Microgrid Systems by Considering Revenue Maximization

MUSTAFA CAGATAY KOCER[1], AHMET ONEN[2,3], (Member, IEEE), JAESUNG JUNG[4], (Member, IEEE), HAKAN GULTEKIN[5], AND SAHIN ALBAYRAK[1]

[1]Department of Electrical Engineering and Computer Science, Technical University of Berlin, 10587 Berlin, Germany
[2]Department of Electrical–Electronics Engineering, Abdullah Gül University, 38080 Kayseri, Turkey
[3]Department of Electrical and Computer Engineering, College of Engineering, Sultan Qaboos University, Al-Khoud, Muscat 123, Oman
[4]Department of Energy Systems Research, Ajou University, Suwon 16499, South Korea
[5]Department of Mechanical and Industrial Engineering, College of Engineering, Sultan Qaboos University, Al-Khoud, Muscat 123, Oman

Corresponding author: Jaesung Jung (jjung@ajou.ac.kr)

This research was supported by Energy AI Convergence Research & Development Program through the National IT Industry Promotion Agency of Korea (NIPA) funded by the Ministry of Science and ICT (No. S1601-20-1005).

ABSTRACT The radical increase in the popularity of electric vehicles (EVs) has in turn increased the number of associated problems. Long waiting times at charging stations are a major barrier to the widespread adoption of EVs. Therefore, battery swapping stations (BSSs) are an efficient solution that considers short waiting times and healthy recharging cycles for battery systems. Moreover, swapping stations have emerged as a great opportunity not only for EVs, but also for power systems, with regulation services that can be provided to the grid particularly for small networks, such as microgrid (MG) systems. In this study, the optimum location and size that maximize the revenue of a swap station in an MG system are investigated. To the best of our knowledge, this study is first to solve the placing and sizing problem in the MG from the perspective of a BSS. The results indicate that bus 23 is the BSS's optimal location and is crucial for maximizing revenue and addressing issues like the provision of ancillary services in microgrid system. Finally, the swap demand profile of the station serving electric bus public transportation system was obtained using an analytical model based on public transportation data collected in Berlin, Germany.

INDEX TERMS Ancillary services, battery swapping station, electric bus, electric vehicle, microgrid, optimal location.

I. INTRODUCTION

Growing awareness of the adverse effects of climate change and efforts to reduce greenhouse emissions have increased the popularity and reputation of electric vehicles (EVs). However, numerous problems, such as the high cost of battery degradation are factors that deter potential EV customers [1]. The long charging time of EVs, particularly compared to that of refueling vehicles with internal combustion engines, is a problem hindering the prevalence of EVs [2], [3]. Although fast-charging stations present a feasible solution in this regard, the degradation that occurs in batteries during fast charging indicates that these stations cannot be considered as the best solution [4]. In recent years, battery swapping stations (BSSs) have become increasingly desirable as reliable solutions [5].

BSSs have the technological infrastructure that enable EV owners to replace discharged batteries in under a minute. By the virtue of saving time, unlike charging stations, BSSs have the potential to compete with gasoline stations [6], [7]. The benefits provided by BSSs are not limited to EVs. With the implementation of vehicle-to-grid (V2G) approaches, BSSs provide various regulation services to the grid with their battery stacks. In addition, the flexible planning of battery charging times means that the BSS does not generate extra stress on the grid during peak load periods and offers

The associate editor coordinating the review of this manuscript and approving it for publication was N. Prabaharan.

a cost-effective solution for both itself and the power system [8]. The possibility of charging the batteries for a long period instead of fast charging prevents a rapid decline in their state of health. Thus, a high lifecycle number can be achieved. Considering the limited number of materials required by batteries, BSS is a greener solution than a charging station in terms of sustainability [9], [10].

V2G technology is a promising solution for the ancillary service needs of networks with a high renewable penetration. However, the distributed and stochastic characteristics of V2G systems make them difficult to control [11]. The BSS makes the entire V2G organization manageable and simple because it completely eliminates the aggregator required to establish communication between EVs and grid operators. Therefore, the BSS facilitates the provision of ancillary services by centrally controlling several batteries.

Moreover, the responsibility of a BSS is great for small-scale networks that depend on renewable energy, such as microgrids (MGs). In such systems, it is extremely difficult to provide voltage stability against fluctuations caused by renewable-based generation and to achieve high service quality [12], [13]. In such a case, the contribution of the BSS for satisfying the demand facilitates the adaptation of MG systems.

A. LITERATURE REVIEW

The majority of studies on BSSs are based on various approaches developed for cost optimization of charging operations. An optimization model for BSS was presented in one of the first studies on BSS [6]. The authors considered the swap demand uncertainty and day-ahead planning to model the optimization problem. An optimization problem was solved in [14] to minimize the BSS operation cost. A model that analyzes the battery swap behavior of EV owners based on a real survey study and proposes an appropriate optimum charging mode is given in [15]. The authors of [16] presented an operational strategy for a prosumer BSS that considered service availability and self-consumption of photovoltaic (PV) power. In [17] and [9], the optimum charging schedule of BSS serving electric buses (EBs) was examined. In addition, [18] aims to minimize the total single-day cost of a battery swapping station serving EBs by considering the demand response. In another study [19], the effect of replacing charging stations with BSS on the power system is examined in a 32-bus system.

Reference [20] presented the optimal strategy of a MG and BSS as two independent stakeholders with conflicting goals. Reference [21] developed a bi-level optimization program that maximizes the profit of the BSS at a low level and reduces the cost of the MG at a high level. Another study [22] presented a bi-level model, where a solution system that optimizes the islanded MG at the upper level while reducing the cost of the BSS at the lower level was executed. Reference [23] proposed a Lyapunov optimization framework based on queueing theory for a real-time energy management strategy for a BSS-based MG. In addition, in [24], the operating cost of the MG was minimized by utilizing the BSS for a grid-connected MG with PV and wind turbines

Few studies have been conducted on the placement and sizing of BSSs. Placement and sizing studies have mostly been conducted for charging stations. Nevertheless, researchers have benefited from these studies. Reference [25] solved the charging station siting problem in a system that includes renewable generation and storage assets. An optimum location study involving a real case was completed in [25], and detailed network constraints were considered in this study. In addition, various studies on the placement of charging stations in distribution networks can be found in the literature [27], [28], [29], [30], [31]. Reference [32] is one of the first studies conducted on the optimum placement problem of BSSs. The authors determined the most suitable location and size for BSS using the artificial bee colony method. The study aimed to determine the location where the power loss for the network is the lowest. In another study [33], the optimal siting and sizing problem for a system with distributed generation and BSS was solved. To date, only one study [34] has been conducted that considered BSSs as a solution for the sitting problem in MGs. The authors obtained optimum placement of the BSS in a microgrid system. However, the sitting problem is solved only from the perspective of a microgrid. In addition, no swap demand analysis was performed for the BSS. The study aimed at reducing the operational cost of MGs. Finally, no previous study has addressed BSS placement problems and economic analysis.

The literature on placement problems has primarily focused on solving problems related to charging stations, whereas the placement of BSS is a relatively new and under-explored research area. Solving the placement problem of BSS in various systems is crucial for ensuring the effective integration of BSS with existing power systems. Therefore, there is a need for more research in this area to address the placement challenges of BSS and enhance its integration with power systems, especially with small networks such as MG. Details are given in Table 1. The existing literature on the placement of BSS in MG has primarily focused on assessing the overall benefits of such placements on the MG or distribution network. However, there is a noticeable research gap in investigating BSS placement in MG from the perspective of the BSS itself. Specifically, the current literature has not adequately investigated the effects of the unique features of BSS on the optimal placement within the MG to enhance BSS's economic, operational efficiency, and reliability. Therefore, there is a critical need to focus on the BSS placement in MG from the BSS's perspective to fill this research gap and to improve the performance of BSS in the MG.

B. CONTRIBUTION OF THE PAPER

In this study, the siting and sizing problems of the BSS in a MG system are solved. The main contributions of this study are as follows:

TABLE 1. Comparison of related studies.

Study	Research Gap	Research Topic	Methodology
[6], [14]-[19]	The placement problem has not been studied.	Optimization of BSS operation	Novel optimization/strategy models for BSS operation.
[20]-[24]	The placement of BSS has not been investigated.	Operation of MG system with BSS	Bi-level optimization frameworks and energy management strategies for MG and BSS.
[25]-[31]	Only the placement of charging stations has been investigated, while BSS placement has not been studied.	Optimal charging station placement	Novel hybrid algorithms, particle swarm optimization and mixed integer linear programming methods for optimum charging station placement
[32]-[34]	The placement of BSS has been studied primarily from the perspective of the overall benefit to MG or distribution network. There is a research gap in investigating BSS placement in MG from the perspective of the BSS itself.	Optimal BSS placement	Mixed-integer nonlinear optimization and novel hybrid algorithms.

1) This is the first work to address the optimum placement of BSSs in a MG from the perspective of the BSS. The authors prioritize revenue maximization of the BSS. Accordingly, the income to be obtained from swap operations and regulation service capacity maximization is considered, along with the location problem. Case studies were conducted on a MG system operating in a grid-connected system.
2) The placement problem is combined with an economic analysis, such as the return on investment (ROI). Therefore, the results are discussed in terms of techno-economic projection.
3) The paper formulates an optimization problem that considers multiple factors that impact the performance of the system, including constraints related to both the BSS and battery level, in addition to constraints related to optimal power flow (OPF). This comprehensive optimization approach ensures a better understanding of the performance of the system.

C. ORGANIZATION OF THE PAPER

The remainder of this paper is organized as follows. Section II describes the MG and BSS organization. Section III presents the problem formulation, which includes the swap demand and an optimization model. The solution methodology is presented in Section IV. In Section V, the results are presented to the reader. Finally, Section VI concludes the paper.

II. MICROGRID AND BSS

This section provides information about the MG and BSS used in the study. Specifically, the assets and operations of these systems are explained.

A. MICROGRID ASSETS

MG systems provide a suitable environment for the utilization of renewable energy resources (RERs) owing to their easily controllable small size. However, owing to the stochastic nature of RERs, MG systems cause unpredictable circumstances [35]. Therefore, the use of RERs with different characteristics may create cases in which they address each other's deficiencies. In this study, PV and wind sources were included in the microgrid system. Although PV and wind power are low-emission and viable solutions in terms of sustainability, a MG system in islanding mode requires more additional sources. In this study, the MG continued its operations in islanding mode without any problems since thermal distributed generators (DGs) that assist RERs were added to the system. The responsibilities of these generators are critical, particularly to satisfy reactive loads.

B. BSS ORGANIZATION

As an innovative solution, the BSS provides a battery swap service to EVs at a fee. For the BSS to offer these services, the EV design should be compatible with the replaceable battery. Once the energy stored in a battery drops below a certain state-of-charge (SoC) level, EVs can replace their batteries with fully charged batteries at the station. The discharged batteries are centrally controlled by the BSS and recharged at specified time intervals. Fully charged batteries are prepared for swap operations or regulation services to be provided to the grid according to the decision mechanism of the BSS. The BSS operations in this study are based on three assumptions. (1) Only fully charged batteries can be included in swap or regulation operations, and the BSS can provide both services in the same timeframe. (2) In the model, the time required for the swap process is neglected and the batteries are charged for the demand in the next period. (3) The battery capacity of the BSS was fixed, and the charging and discharging processes of the batteries were performed with constant power.

The relationship of the BSS with the power grid creates opportunities for both parties. With the aid of the regulation services it provides, the BSS increases its revenue, reinforces

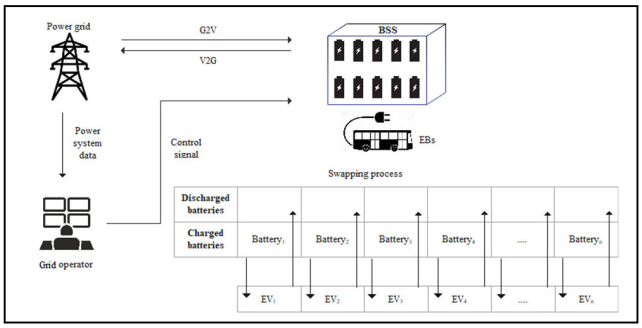

FIGURE 1. BSS operation and its interaction with the power grid.

the network, and tolerates the disadvantages generated during the charging schedule. It monitors the control signals of the grid operator and the swap demand plan of the EBs throughout the day, so that the operation runs smoothly. Figure 1 illustrates the BSS operation and its interaction with the power grid.

BSS has the following options for increasing revenue: The BSS satisfies the demand for swap operations without any problems. In addition, the BSS charges its batteries at low electricity prices and profits from regulation services by selling energy to the MG when prices are high. These two methods are critical elements that determine the profit maximization of a BSS.

III. PROBLEM FORMULATION

The problem formulation consists of two steps. In the first stage, the EB consumption model is introduced. In the second stage, an optimization model for profit maximization of the BSS is presented.

A. BATTERY SWAP DEMAND MODEL

In this section, the model developed for calculating the battery swap demand that the BSS must satisfy is presented. Note again that the BSS serves EBs operating in Berlin public transport services. The calculations were based on actual data.

To obtain the swap demand, the energy consumed by each EB during the trip from one terminus to the other was calculated. First, the energy consumed by each EB between two consecutive stops is obtained using a detailed analytical method. Subsequently, the battery swap demand profile that the BSS needs to satisfy in a 24-hour period is attained using the data on the number of stops on each bus line and the number of trips they complete daily.

In this section, we describe how to model the energy consumed by EBs during their duty periods. A detailed energy demand model was used to evaluate the consumed energy ''terminus-to-terminus'' in a bus route by calculating the energy consumption between two consecutive bus stops. The energy consumption model between two consecutive bus stops mapped in this section is based on a prevalent longitudinal dynamics model [9], [36], [37].

The tractive force F_{tr} is given by the following equation:

$$F_{tr} = F_{drag} + F_{roll} + F_{climb} + F_{inertia} \tag{1}$$

The term $F_{drag} = K_d v^2$ states the aerodynamic drag force, where $K_d = 0.5\rho C_d A$. The density of air is expressed by ρ with units of kg/m^3. The term C_d denotes the drag coefficient, A indicates the frontal area of the vehicle in m^2, and v refers to the speed of the vehicle in m/s. The expression $F_{roll} = Mgfcos(\alpha)$ represents the rolling friction, and f indicates the rolling resistance coefficient. The equation $F_{climb} = Mgsin(\alpha)$ represents the grade force. M denotes the mass of the vehicle in kilograms, g denotes the acceleration due to gravity (9.81 m/s^2), and α symbolizes the gradient of the road. The force of inertia is given by $F_{inertia} = \delta Ma$, which is the result of changes in the stored kinetic energy owing to acceleration and deceleration. The expression a is the acceleration of the vehicle, and δ corresponds to a factor that models the inertia of the rotating components in the drivetrain.

If data on the number of in-vehicle passengers are available, the total mass of the vehicle can be assessed as $M = M_{curb} + n_{pax}m_{pax}$. M_{curb} represents the curb weight of the vehicle, n_{pax} is the number of passengers, and m_{pax} the weight of the passenger. The term E_{tr} states the energy demand due to the tractive force between two consecutive bus stops, which is evaluated as follows:

$$E_{tr} = \int \eta(K_d v\,(t)^2 + Mgfcos(\alpha) + Mgsin(\alpha) + \delta Ma(t))v(t)dt \tag{2}$$

The term η is an efficiency factor used for losses in the inverter, motor, and drivetrain. When the vehicle brakes ($a\,(t) < 0$), the tractive force has a negative value. During braking, the EV stores kinetic energy via regenerative braking. Hence, η is determined separately, based on the sign of the tractive force.

$$\eta = \begin{cases} \frac{1}{\eta_t \eta_{PE} \eta_m}, & F_{tr}\,(t) \geq 0 \\ r_{reg}\eta_t \eta_{PE} \eta_m, & F_{tr}(t) < 0 \end{cases} \tag{3}$$

The term η_t represents the drivetrain and gearbox efficiency, η_{PE} indicates the inverter efficiency, η_m denotes the motor efficiency, and r_{reg} refers to the regeneration factor.

To determine the energy consumption of the EB, a driving profile between consecutive stops of the bus route should be developed. Therefore, the method proposed in [37] was used to create a driving profile. A trip between two consecutive stops involves $\eta_h + 1$ phases of length $D' = D/(\eta_h + 1)$. The term η_h represents the number of intermediate halts between two bus stops, such as stops at traffic lights. The first section begins with an constant acceleration a_+ over distance d_0, followed by a constant coasting speed v_1 over distance d_1 and ends with constant deceleration a_- over distance d_2, yielding the relation $d_0 + d_1 + d_2 = D'$. Figure 2 illustrates the trip profiles for two consecutive stops.

For simplicity, it is assumed that there is only one intermediate halt point between two stops, that is, $\eta_h = 1$, and

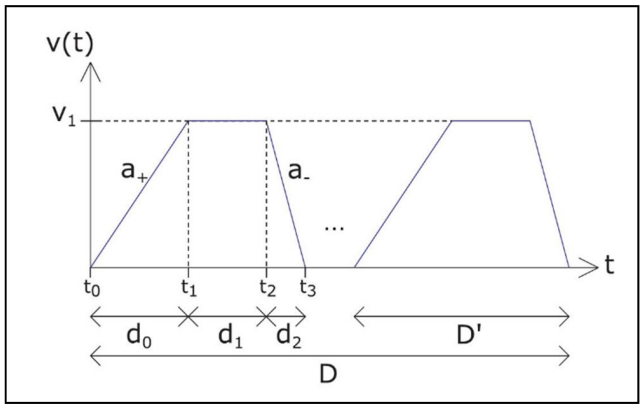

FIGURE 2. Trip profile between two consecutive stops [36].

that the coasting speed between the two stops is equal to $v_1 = 1.5v_{avg}$. The simplified velocity profile eliminates the time component in (2). Thus, E_{tr} is only subject to the known parameters for each phase, given by

$$\begin{aligned} E_{tr} &= (\eta_h + 1)\, E'_{tr} \\ &= (\eta_h + 1) \\ &\quad \times (E'_{tr,a(t)=a_+} + E'_{tr,a(t)=0} + E'_{tr,a(t)=a_-}) \quad (4) \\ E'_{tr,a(t)=a_+} &= \eta d_0 (Mgfcos(\alpha) + Mgsin(\alpha) \\ &\quad + K_d a_+ d_0 + \delta M a_+) \quad (5a) \\ E'_{tr,a(t)=0} &= \eta d_1 (Mgfcos(\alpha) + Mgsin(\alpha) + K_d v_1^2) \quad (5b) \\ E'_{tr,a(t)=a_-} &= \eta d_2 (Mgfcos(\alpha) \\ &\quad + Mgsin(\alpha) - K_d a_- d_2 + \delta M a_-) \quad (5c) \end{aligned}$$

$$d_0 = \frac{v_1^2}{2a_+} \quad (6a)$$

$$d_1 = D' - (d_0 + d_2) = D' - \frac{v_1^2}{2}\left(\frac{1}{a_+} - \frac{1}{a_-}\right) \quad (6b)$$

$$d_2 = D' \frac{a_+}{a_+ - a_-} \quad (6c)$$

The energy demand between consecutive bus stops (E^{trip}_{total}) is expressed as

$$E^{trip}_{total} = E_{tr} \quad (7)$$

The terminus-to-terminus energy demand ($E^{journey}_{total}$) is given by the sum of the energy consumption of each individual stop-to-stop trip, which is expressed as

$$E^{journey}_{total} = \sum_{trip} E^{trip}_{total} \quad (8)$$

For ease of exposition, we tabulated the values of the parameters listed in this subsection in Table 2.

B. BSS MODEL

The BSS model was developed for profit maximization. To increase revenue, the BSS must optimize its operation schedule. In this study, the objective function was defined as

TABLE 2. Parameters in swap demand calculation of BSS.

Parameter	Value	Unit
C_d	0.7	-
ρ	1.18	kg/m^3
f	0.008	-
η_t	0.97	-
η_{PE}	0.95	-
η_m	0.91	-
δ	1.1	-
r_{reg}	0.6	-
m_{pax}	75	kg
a_+	1	m/s^2
a_-	-1.5	m/s^2
n_{pax}	10	-
M_{curb}	12.5	t
A	8.3	m^2
D	400	m
v	16.7	km/h
η_h	1	-

mixed-integer programming. The objective function is given in (9) and consists of three components. These components include the income from swap operations, charging costs, and regulation service income.

$$\begin{aligned} max\ \boldsymbol{F_1} = &\sum_{t=1}^{T} \boldsymbol{P_{B,dc,t}}\, \lambda - \sum_{t=1}^{T} \boldsymbol{P_{B,ch,t}}\, \lambda \\ &+ \omega_{swp} \boldsymbol{C_{bat}} \sum_{t=1}^{T} \boldsymbol{N_{EB,t}} \end{aligned} \quad (9)$$

In the above equation, λ symbolizes the day-ahead electricity prices for buying and selling electricity. C_{bat} denotes the energy capacity required to fully charge the battery. $N_{EB,t}$ indicates the number of EBs arriving at the station to swap in period t. $P_{B,dc,t}$ denotes the power discharged for the regulation services in time interval t. Similarly, $P_{B,ch,t}$ is the power used to charge the batteries in time frame t. ω_{swp} symbolizes the battery swap price for EBs. T denotes the total number of hours per day, and t indicates the scheduling timeframe in hours.

The constraints of the objective function are created for BSS and battery components.

$$\boldsymbol{C_{B,t+1}} = \boldsymbol{C_{B,t}} + \eta_{B,ch}\, \boldsymbol{P_{B,ch,t}}\, \Delta \boldsymbol{t} - \frac{\boldsymbol{P_{B,dc,t}}}{\eta_{B,dc}} \Delta \boldsymbol{t} \quad \forall \boldsymbol{t} \quad (10)$$

Equation (10) models the impact of charging, regulation, and swap operations performed in period t on the available capacity in period $t+1$. $C_{B,t}$ and $C_{B,t+1}$ indicate the available capacity of the BSS at time frames t and $t+1$, respectively. Δt denotes the time duration. In addition, the charging and discharging efficiencies are represented by $\eta_{B,ch}$ and $\eta_{B,dc}$.

$$0 \le P_{B,ch,t} \le P_{B,ch,max} \quad \forall t \quad (11)$$

$$0 \le P_{B,dc,t} \le P_{B,dc,max} \quad \forall t \quad (12)$$

Maintaining charge and discharge rates within a certain range is crucial for power system stability and battery health. Equations (11) and (12) subject the BSS to this range. $P_{B,ch,max}$ and $P_{B,dc,max}$ denote the charging and discharging limits, respectively.

$$C_{B,min} \leq C_{B,t} + \eta_{B,ch} P_{B,ch,t} - \frac{P_{B,dc,t}}{\eta_{B,dc}} \leq C_{B,max} \quad (13)$$

The total capacity of the BSS must be within specified limits. Equation (13) presents the constraint developed for this case. $C_{B,min}$ and $C_{B,max}$ represent the minimum and maximum capacities of BSS, respectively.

$$\boldsymbol{C_{B,min} \leq \sum_{t=1}^{T} (\eta_{B,ch} P_{B,ch,t} - \frac{P_{B,dc,t}}{\eta_{B,dc}}) + C_{B,0} \leq C_{B,max}} \quad (14)$$

Equation (14) ensures that the BSS continues its activities within the determined capacity limits during the entire scheduling period, considering the initial capacity of the BSS. Moreover, $C_{B,0}$ denotes the initial capacity of the BSS at the beginning of the scheduling horizon.

$$\boldsymbol{D_{B,t+1} \leq C_{B,t} + \eta_{B,ch} P_{B,ch,t} - \frac{P_{B,dc,t}}{\eta_{B,dc}}} \quad (15)$$

In addition, the main responsibility of the BSS is to keep swap operations running smoothly. The remaining capacity after the operation of the BSS at time t must meet the demand at time $t+1$. Therefore, (15) secures this, and $D_{B,t+1}$ represents the next-hour swap demand.

$$\boldsymbol{0 \leq P_{B,reg,t} \leq C_{B,t} - D_{B,t+1} \quad \forall t \in T_{reg}} \quad (16)$$

Equation (16) ensures that the BSS does not exceed its available capacity and meets the demand of the next time period while contributing to ancillary services. $P_{B,reg,t}$ symbolizes the regulation capacity at time t. T_{reg} indicates all the time periods BSS allocates to regulation services.

$$N_{bat,ful,t} + N_{bat,emp,t} + N_{bat,ch,t} + N_{bat,dc,t} = N_{bat} \quad \forall t \quad (17)$$

Equation (17) represents the total number of batteries in the BSS. $N_{bat,ful,t}$ and $N_{bat,emp,t}$ indicate the number of fully charged and fully discharged batteries in time frame t, respectively. $N_{bat,ch,t}$ and $N_{bat,dc,t}$ correspond to the number of batteries being charged or discharged, respectively. N_{bat} denotes the total number of batteries.

$$N_{bat,ch,t} \leq N_{bat,pos,\max}, N_{bat,dc,t} \leq N_{bat,pos,\max} \quad \forall t \quad (18)$$

The number of batteries being charged or discharged did not exceed the total battery chargers/dischargers in BSS. where $N_{bat,pos,\max}$ states the total number of chargers/dischargers.

$$C_{bat,t+1} = C_{bat,t} + (\eta_{ch} P_{bat,ch,t} - \frac{P_{bat,dc,t}}{\eta_{dc}}) \Delta t \quad \forall t \quad (19)$$

The charge/discharge constraint of a battery according to the time period is given in (10). $C_{bat,t+1}$ and $C_{bat,t}$ indicate the battery capacities at t+1 and t, respectively. $P_{bat,ch,t}$ and $P_{bat,dc,t}$ represent the charging and discharging powers of a battery in period t, respectively.

$$C_{bat,\min} \leq C_{bat,t} \leq C_{bat,\max} \quad \forall t \quad (20)$$

$C_{bat,\min}$ and $C_{bat,\max}$ denote the minimum and maximum battery capacity, respectively.

IV. SOLUTION METHODOLOGY

In this study, the optimum location and size were investigated for profit maximization of a BSS in a microgrid. This is a power system planning problem and is closely related to power system stability. Therefore, some limitations have been considered for the power balance of the microgrid model, such that the location where the BSS is placed does not cause any problems during operation.

$$V_{min,i} \leq V_{i,t} \leq V_{max,i} \quad \forall i, \forall t \quad (21)$$

Equation (21) ensures that the voltage of each bus is within the limits. $V_{min,i}$ and $V_{max,i}$ are the minimum and maximum bus voltage levels allowed for bus i, respectively. $V_{i,t}$ refers to the voltage of the bus at t.

$$P_{grid,min} \leq P_{grid,t} \leq P_{grid,\max} \quad \forall t \quad (22)$$

The power supplied from the grid was constrained using (22). $P_{grid,max}$ and $P_{grid,min}$ denote the maximum and minimum values, respectively. $P_{grid,t}$ indicates the power purchased from the grid at t.

$$P_{min,j} \leq P_{j,t} \leq P_{max,j} \quad \forall j, \forall t \quad (23)$$

$$Q_{min,j} \leq Q_{j,t} \leq Q_{max,j} \quad \forall j, \forall t \quad (24)$$

The active and reactive power output ranges of the thermal DGs are limited by (23) and (24). $P_{max,j}$ and $Q_{max,j}$ state the maximum active and reactive power outputs, $P_{min,j}$ and $Q_{min,j}$ represent the minimum active and reactive power outputs. j indicates the index number for the thermal DG. $P_{j,t}$ and $Q_{j,t}$ represent the active and reactive power of the j-th thermal DG, respectively.

$$0 \leq P_{w,t} \leq P_{w,\max} \quad \forall t \quad (25)$$

$$0 \leq P_{pv,t} \leq P_{pv,\max} \quad \forall t \quad (26)$$

Equations (25) and (26) constrain the wind and PV power output, respectively. $P_{w,t}$ indicates the power generated by the wind power at time frame t, and $P_{w,\max}$ symbolizes the maximum output. $P_{pv,t}$ indicates the generated PV power in period t and $P_{pv,\max}$ denotes the maximum level.

The problem-solving process is illustrated in Figure 3. The solution steps are as follows:

Step 1: MG is modeled according to the constraints (21)–(26).

Step 2: Define the initial parameters of the MG.

Step 3: BSS is modeled according to (9)–(20).

Step 4: Define the initial parameters of the BSS.

Step 5: BSS chooses a location.

Step 6: BSS determines a size.

Step 7: BSS optimizes charging–discharging schedule.

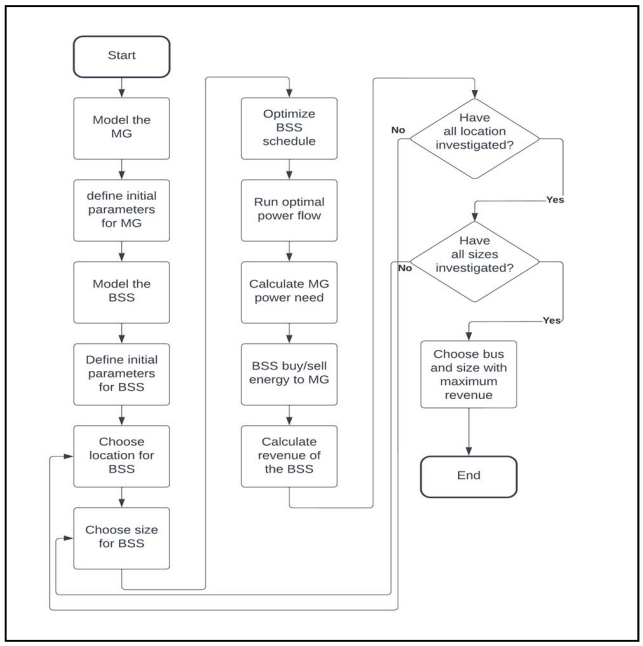

FIGURE 3. Flowchart of the solution.

Step 8: Optimal power flow is executed.
Step 9: MG power requirement is calculated.
Step 10: BSS buys/sells energy to the MG.
Step 11: Revenue of the BSS is calculated.
Step 12: Have all BSS sizes been investigated? If not, return to Step 6.
Step 13: Have all the MG buses been investigated? If not, return to Step 5.
Step 14: Select the bus and size that maximizes the revenue of the BSS.

V. RESULTS

To obtain the results of this study, an MG was designed based on the IEEE 33-bus system. The MG comprises 33 buses, 32 branches, 3 thermal DGs, PV units, 1 wind unit, and fixed loads. The objective is to identify the optimal location of the BSS that maximizes its revenue. Therefore, it is necessary to choose a location that will minimize the cost of the BSS charging operations and enable it to generate high income from regulation services. The data of the IEEE 33-bus system are provided in [38]. A single-line diagram of the MG is illustrated in Figure 4. The location and size details of thermal DGs, PVs, and wind power are shown in Table 3 and Figure 5, respectively. Moreover, the load data is given in Figure 5. The base voltage of the system is 12.66 kV, and the voltage range of the buses is 0.9–1.1 pu.

To demonstrate the effectiveness of the energy consumption model, the swap demand that the BSS must meet is created using 50 EBs assumed to serve in public transportation bus services (PTBS). The routes of EBs were different. They were obtained using data from the PTBS in Berlin, Germany, and the consumption model was tested with real data. The

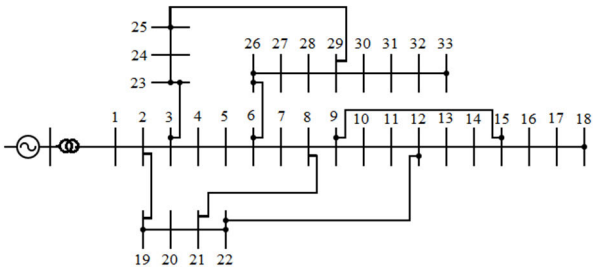

FIGURE 4. MG single line diagram.

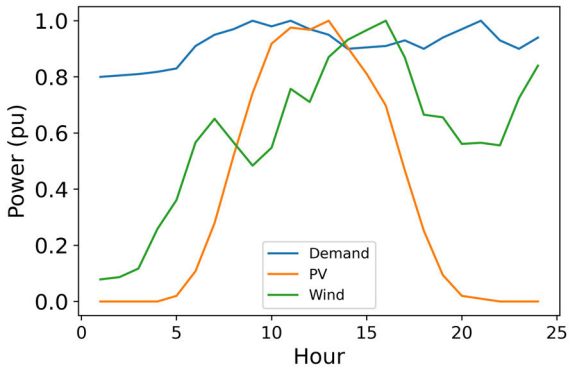

FIGURE 5. Data of demand, PV and wind generation [34].

TABLE 3. Capacity and location of units.

Unit	Location	Power (kW/kVar)
PV #1	18	600 kW
PV #2	20	500 kW
Wind	10	700 kW
Thermal DG #1	3	1500 kW / 1000 kVar
Thermal DG #2	28	1500 kW / 1500 kVar
Thermal DG #3	15	2000 kW / 1500 kVar

battery capacity of the EB was 337 kWh [39]. The chargers in the BSS were assumed to have a charging power of 150 kW. The number of chargers in the BSS varies according to the buses. Since the aim of BSS is to maximize its profit, these data are given in the following sections according to each bus. The scheduling horizon of the case study was 24 h, from midnight to midnight, and the resolution was 1 h. At the beginning of the scheduling horizon, all EBs begin to serve with a full battery, whereas the BSS has zero energy capacity. In addition, the EB swaps the battery when its SoC drops to 5–10%.

As stated in the previous sections, the optimization problem and optimum power flow were created and solved using MATLAB and MATPOWER.

A. BATTERY SWAP DEMAND

The swap demand is computed using the consumption model explained in Section III. The results are depicted in Figure 6.

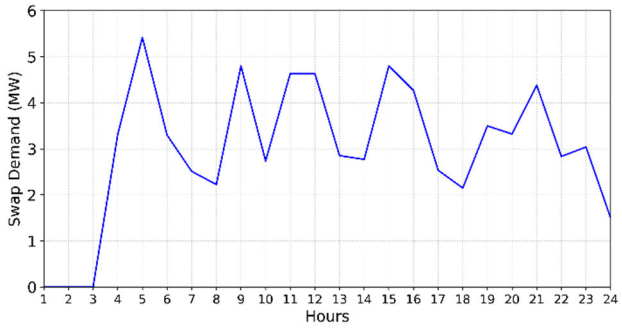

FIGURE 6. Daily battery swap demand for BSS.

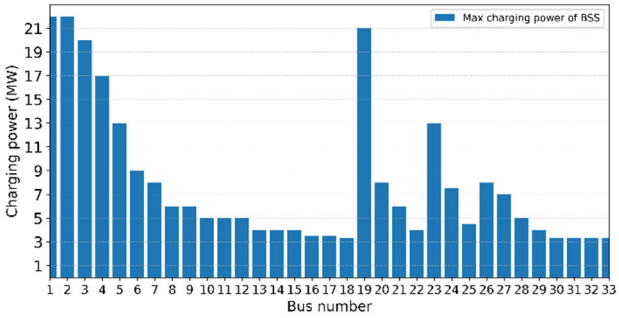

FIGURE 7. Maximum charging power of BSS for each bus in the MG system.

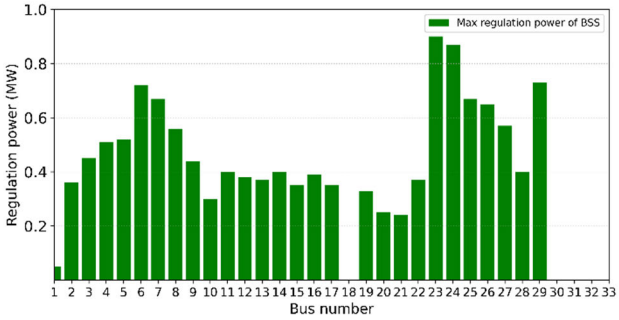

FIGURE 8. Maximum amount of regulation provided by BSS at a resolution of 1 h.

The demand increases in the morning and evening hours at stations serving EVs.

However, in this study, a different pattern appears in the graph, as the BSS serves the EBs operating for the PTBS. These results are in line with the authors' expectations, as each EB may have a different route, timetable, number of stops, or trip duration. The EBs run for 24 h in a regular operation plan. Therefore, the swap demand, which follows a fluctuating profile throughout the day, stands out. The hourly demand varies between 5.4 MW and 0 MW. The average hourly swap demand is 3 MW. The EBs begin with a fully charged battery at the start of the scheduling horizon. There is no swap demand for the first 3 h. Subsequently, the demand increases, and the highest demand occurs at 5 h. A pattern of similar ups and downs was followed until 20 h. After 20 h, a downward trend was observed in the swap demand. The reason for this is the decrease in the number of EBs required as a result of the sparseness of the PTBS at night. During the day, the BSS receives over 300 swap demands from 50 different EBs, and a total of 71535 KW charging capacity is generated from these batteries.

B. OPTIMAL LOCATION OF BSS

In this study, the location that maximizes the revenue of a BSS is investigated. To increase the income, the BSS optimizes the charging–discharging schedule by considering the variability of daily electricity costs. For successful optimization, an upper limit must be set for the charging–discharging power of the BSS. These values vary for each MG bus. The maximum load that the BSS creates in each bus is examined separately. These loads are the highest values that enable the optimal power flow to operate without any problems. To simplify the work, the extra load that the BSS can add during peak load is calculated, which is considered as the maximum charging power of the BSS for a time frame of 1 h. This is crucial for the BSS to complete its charging operations at minimum cost. The maximum charging power of the BSS for each bus is shown in Figure 7.

The figure shows that the highest values are obtained for the 1st and 2nd buses. This is because the system is connected to the main grid via bus 1. The loads created here easily provide the energy required for consumption from the main grid without causing voltage imbalances. Bus 2 is in a balanced position, as it is located in the middle of the grid connection on the first bus and the thermal DG on bus 3. Therefore, this bus is expected to reach a charging power of 22 MW. Bus 3 easily responds to the high demand that may occur in this bus with its thermal DG. From this point onwards, the values decreased. To avoid creating an imbalance in the system while moving away from the grid, the maximum charging power allowed by the optimal power flow decreases regularly until bus 18, and in this bus, the level drops by 3.3 MW. Owing to the connections of buses 19 and 23 with buses 2 and 3, high levels can be reached again at these locations. Although the thermal DG in bus 28 plays an active role in balancing the nearby buses, the rating decreases to 3.3 MW in the last bus of the system.

In Figure 8, the maximum amount of regulation provided by the BSS at a resolution of 1 h in line with the demand from the MG is shown. This is not the total regulation provided at the end of the scheduling horizon, instead, only the highest regulation amounts are observed in the 1 h period. These values are the regulation upper limits used to maximize revenue by optimizing the daily operation of the BSS. Additionally, the BSS provides regulation services with the same day-ahead electricity prices as the grid and thermal DGs. There is not as much difference between the buses, as observed in the maximum charging power. The result of the optimal power

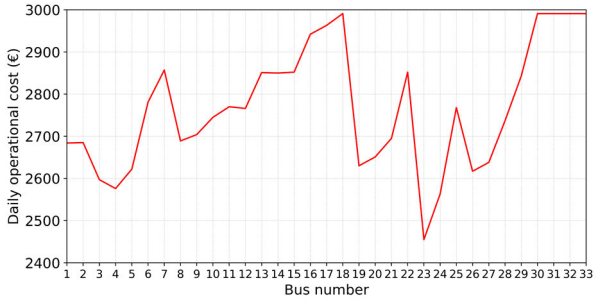

FIGURE 9. Daily operational cost of optimized BSS's for each bus.

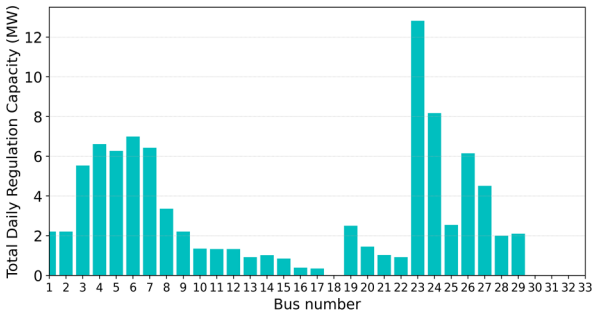

FIGURE 10. Total regulation capacity provided by BSS for a 24 h period.

flow demonstrates that the maximum values were achieved at busbars 23 and 24. This provides a projection of the total revenue that can be obtained from the provision of ancillary services. However, for this, the BSS schedule must be optimized, and each hour of the day must be carefully studied. Since the charging power of buses 18, 30, 32, 32, and 33 is low, they only have sufficient charging capacity to satisfy the swap demand. Therefore, the regulation capacity was zero for these buses.

The income from swap operations is considered to be equal for all buses. The BSS must satisfy the same swap demand for each bus. The daily operational cost of the BSS is obtained by subtracting the regulation income from the charging costs. Figure 9 presents the daily operational cost of the optimized charging and regulation operations of the BSS according to the buses without considering swap income. The graph clearly shows that the daily operating cost of the BSS is the lowest on bus 23. Although the BSS placed on bus 23 does not have the highest charging power, it can offer more regulation services because of its locational advantage. This is crucial for reducing operational costs. The daily operational cost of the BSS on bus 23 was 2455 euros. The second lowest cost is on bus 24, at 2563 euros. Buses 18, 30, 31, 32, and 33 have the highest costs. Since these buses have low charging power, they cannot allocate capacity for regulation services. Their daily operational cost is approximately 3000 euros.

Revenue from regulation services is crucial for reducing operational costs. Figure 10 presents the total regulation capacity provided by the BSS over the course of the day. As expected, the BSS placed on bus 23 is the location where most energy is sold to the MG, with a regulation capacity of 12.82 MW.

In Figure 11, the optimum charging–discharging schedule of the BSS on bus 23 is shown. The figure shows that the BSS charges with maximum charging power (13 MW) at low prices and allocates high price periods for regulation services to reduce operational costs. In this process, the BSS continues the swap operations without any problems. Regulation services present an important opportunity for reducing the operational costs of BSS. Based on the results given, there is a difference of more than 500 euros in daily costs between the buses where the regulation service can and cannot be provided. However, the main source of income for the BSS is

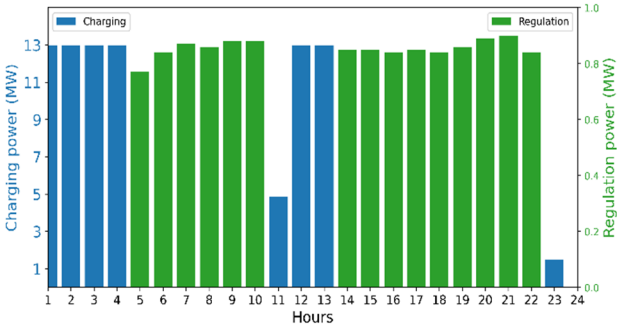

FIGURE 11. Optimum charging-discharging schedule of BSS on bus 23.

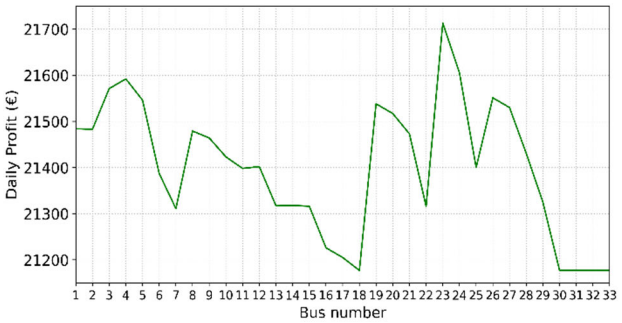

FIGURE 12. Daily profit of BSS on all buses including the income from swap operations.

battery swap operations. According to [40], EV users pay $23 for swapping a 70 kWh battery. This means that $114 should be paid to swap the 337 kWh battery. The BSS completes 212 swap operations during the day. Therefore, the daily income of the BSS from swap operations is 24168 EUR. Since the same swap demand is met for each bus, this amount is accepted for all buses.

Figure 12 shows the daily profit that the BSS obtains on all buses when the income from swap operations is added. The daily profit of the BSS on bus 23 increases to 21713 euros. The average profit earned for all buses is 21400 euros. The difference between the buses with the lowest and highest profit is 536 euros. When this difference is considered on an annual basis, it creates a difference of approximately 200k euros. In a ten-year operational period, the amount reached a difference of approximately 2 million euros. This shows that location selection is an important element of BSS investment.

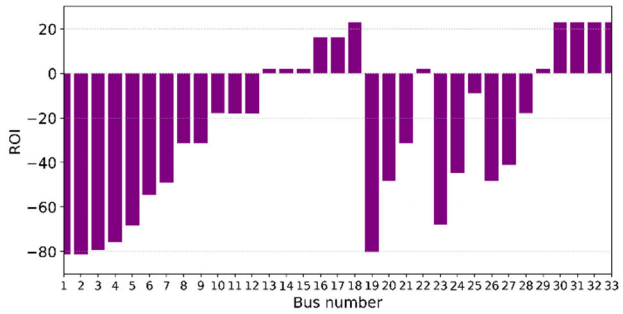

FIGURE 13. ROI values of all buses for 1-year period.

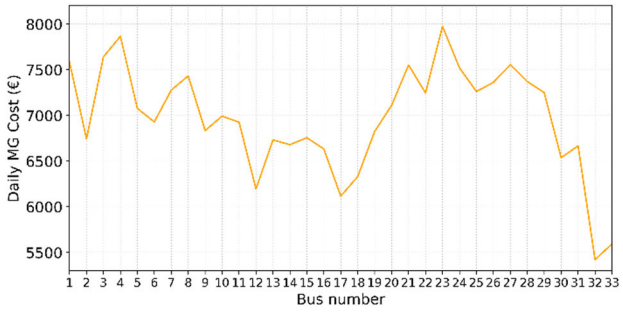

FIGURE 14. Daily operational cost of MG for each bus.

At this point, it seems appropriate to conduct an investment analysis of the BSS. For this analysis, the return on investment (ROI) is a simple and effective method. The ROI formula is given as follows:

$$ROI = \frac{Net\ Return\ on\ Investment}{\text{Cost of Investment}}\ x\ 100\% \qquad (27)$$

An example ROI calculation is performed for the BSS on bus 23. To calculate the ROI, investment costs must be obtained. Reference [41] states the investment cost for a swap station with 50 charging units was $15.7 million. In this study, the BSS on bus 23 has 86 chargers. This shows that the investment cost is $27 million. The example ROI calculation is performed on bus 23 for a one-year operational period. The annual profit of bus 23 is $8,76 million. As a result, the ROI at the end of the one-year period is -67.56%. The ROI values of all the buses for the one-year period are shown in Figure 13. The ROI values of the buses that cannot allocate capacity for regulation are significantly high, as shown in Figure 13. This is because few chargers maintain a very low investment cost.

Upon determining the daily profit and location of the BSS, the operational costs of the MG were calculated, as shown in Figure 14. There is an inverse proportion between the profitability ratio of the BSS and the daily operational cost of the MG. The highest MG operational cost occurred in bus 23. Since bus 23 is the location where the MG requires the most regulation, following the addition of BSS, this caused an increase in the cost of bus 23. Bus 32, which is one of the buses where regulation services are not provided by the BSS, has the lowest MG operational cost. The difference between the highest and lowest MG daily costs is 2553 euros.

VI. CONCLUSION

The BSS concept offers several innovative opportunities for EVs and power systems. Since BSSs have high charging and discharging potential, planning studies on BSS are crucial for many parties. In this study, a methodology is developed to determine the optimal location and size of a BSS to maximize the profit in the microgrid system. The problem has been investigated by considering the energy consumption characteristics of the vehicles with real data. Using an analytics-based model, the swap demand of a BSS serving EBs operating for the PTBS in Berlin is calculated. In the next step, the optimal charging–discharging schedule of the BSS is obtained for different locations and sizes in the 33-bus microgrid. The optimization problem is carefully formulated by incorporating constraints related to both the BSS and battery level, in addition to constraints related to OPF. The resulting formulation ensures a comprehensive optimization approach that takes into account multiple factors that impact the performance of the system. As a result of the optimized 24-hour operation, the location and size at which the BSS attained maximum profit are obtained. In addition, the ROI values of the investment are given over the daily income generated by the BSS from the swap operations and regulation services. It ensures that the decision-making strategy obtained is supported by economic analysis, and the results of the study are evaluated in terms of techno-economics. Finally, the data used in this study were obtained from Berlin, Germany.

REFERENCES

[1] C. Aravena and E. Denny, "The impact of learning and short-term experience on preferences for electric vehicles," *Renew. Sustain. Energy Rev.*, vol. 152, Dec. 2021, Art. no. 111656, doi: 10.1016/J.RSER.2021.111656.

[2] G. Adu-Gyamfi, H. Song, B. Obuobi, E. Nketiah, H. Wang, and D. Cudjoe, "Who will adopt? Investigating the adoption intention for battery swap technology for electric vehicles," *Renew. Sustain. Energy Rev.*, vol. 156, Mar. 2022, Art. no. 111979, doi: 10.1016/J.RSER.2021.111979.

[3] S. Afshar, P. Macedo, F. Mohamed, and V. Disfani, "Mobile charging stations for electric vehicles—A review," *Renew. Sustain. Energy Rev.*, vol. 152, Dec. 2021, Art. no. 111654, doi: 10.1016/J.RSER.2021.111654.

[4] A. Ahmadian, M. Sedghi, A. Elkamel, M. Fowler, and M. A. Golkar, "Plug-in electric vehicle batteries degradation modeling for smart grid studies: Review, assessment and conceptual framework," *Renew. Sustain. Energy Rev.*, vol. 81, pp. 2609–2624, Jun. 2018, doi: 10.1016/J.RSER.2017.06.067.

[5] F. Ahmad, M. Saad Alam, I. Saad Alsaidan, and S. M. Shariff, "Battery swapping station for electric vehicles: Opportunities and challenges," *IET Smart Grid*, vol. 3, no. 3, pp. 280–286, Jun. 2020, doi: 10.1049/iet-stg.2019.0059.

[6] M. R. Sarker, H. Pandžić, and M. A. Ortega-Vazquez, "Optimal operation and services scheduling for an electric vehicle battery swapping station," *IEEE Trans. Power Syst.*, vol. 30, no. 2, pp. 901–910, Mar. 2015, doi: 10.1109/TPWRS.2014.2331560.

[7] *From Three Minutes to 30 Seconds, NIO-Led Battery Swap Mode Sparks Race—CnTechPost*. Accessed: Apr. 8, 2021. [Online]. Available: https://cntechpost.com/2020/10/27/from-three-minutes-to-30-seconds-nio-led-battery-swap-mode-sparks-race/

[8] S. R. Revankar and V. N. Kalkhambkar, "Grid integration of battery swapping station: A review," *J. Energy Storage*, vol. 41, Sep. 2021, Art. no. 102937, doi: 10.1016/J.EST.2021.102937.

[9] M. C. Kocer, O. Yurdakul, and S. Albayrak, "Optimal scheduling of battery swapping stations for electric public transportation," in *Proc. IEEE PES Innov. Smart Grid Technol. Eur. (ISGT Europe)*, Oct. 2021, pp. 1–5, doi: 10.1109/ISGTEUROPE52324.2021.9639941.

[10] M. C. Kocer, C. Cengiz, M. Gezer, D. Gunes, M. A. Cinar, B. Alboyaci, and A. Onen, "Assessment of battery storage technologies for a Turkish power network," *Sustainability*, vol. 11, no. 13, p. 3669, Jul. 2019, doi: 10.3390/su11133669.
[11] F. Gonzalez Venegas, M. Petit, and Y. Perez, "Active integration of electric vehicles into distribution grids: Barriers and frameworks for flexibility services," *Renew. Sustain. Energy Rev.*, vol. 145, Jul. 2021, Art. no. 111060, doi: 10.1016/J.RSER.2021.111060.
[12] M. C. Kocer, Y. Yoldas, S. Goren, A. Onen, I. Alan, S. Al-Agtash, B. Azzopardi, N. Martensen, J. L. Martinez-Ramos, D. Tzovaras, L. Hadjidemetriou, M. Khiat, T. Camilleri, and N. Borg, "Cloud induced PV impact on voltage profiles for real microgrids," in *Proc. 5th Int. Symp. Environ.-Friendly Energies Appl. (EFEA)*, Sep. 2018, pp. 1–6, doi: 10.1109/EFEA.2018.8617080.
[13] Y. Yoldaş, A. Önen, S. M. Muyeen, A. V. Vasilakos, and İ. Alan, "Enhancing smart grid with microgrids: Challenges and opportunities," *Renew. Sustain. Energy Rev.*, vol. 72, pp. 205–214, May 2017, doi: 10.1016/J.RSER.2017.01.064.
[14] H. Wu, G. K. H. Pang, K. L. Choy, and H. Y. Lam, "An optimization model for electric vehicle battery charging at a battery swapping station," *IEEE Trans. Veh. Technol.*, vol. 67, no. 2, pp. 881–895, Feb. 2018, doi: 10.1109/TVT.2017.2758404.
[15] R. Rao, X. Zhang, J. Xie, and L. Ju, "Optimizing electric vehicle users' charging behavior in battery swapping mode," *Appl. Energy*, vol. 155, pp. 547–559, Oct. 2015, doi: 10.1016/J.APENERGY.2015.05.125.
[16] N. Liu, Q. Chen, X. Lu, J. Liu, and J. Zhang, "A charging strategy for PV-based battery switch stations considering service availability and self-consumption of PV energy," *IEEE Trans. Ind. Electron.*, vol. 62, no. 8, pp. 4878–4889, Aug. 2015, doi: 10.1109/TIE.2015.2404316.
[17] P. You, Z. Yang, Y. Zhang, S. H. Low, and Y. Sun, "Optimal charging schedule for a battery switching station serving electric buses," *IEEE Trans. Power Syst.*, vol. 31, no. 5, pp. 3473–3483, Sep. 2016, doi: 10.1109/TPWRS.2015.2487273.
[18] B.-R. Ke, Y.-H. Lin, H.-Z. Chen, and S.-C. Fang, "Battery charging and discharging scheduling with demand response for an electric bus public transportation system," *Sustain. Energy Technol. Assessments*, vol. 40, Aug. 2020, Art. no. 100741, doi: 10.1016/J.SETA.2020.100741.
[19] W. Alharbi, A. S. B. Humayd, R. P. Praveen, A. B. Awan, and V. P. Anees, "Optimal scheduling of battery-swapping station loads for capacity enhancement of a distribution system," *Energies*, vol. 16, no. 1, p. 186, Dec. 2022, doi: 10.3390/EN16010186.
[20] S. Esmaeili, A. Anvari-Moghaddam, and S. Jadid, "Optimal operation scheduling of a microgrid incorporating battery swapping stations," *IEEE Trans. Power Syst.*, vol. 34, no. 6, pp. 5063–5072, Nov. 2019, doi: 10.1109/TPWRS.2019.2923027.
[21] M. Hemmati, M. Abapour, and B. Mohammadi-Ivatloo, "Optimal scheduling of smart microgrid in presence of battery swapping station of electrical vehicles," in *Electric Vehicles in Energy Systems: Modelling, Integration, Analysis, and Optimization*. Springer, Jan. 2020, pp. 249–267, doi: 10.1007/978-3-030-34448-1_10.
[22] Y. Li, Z. Yang, G. Li, Y. Mu, D. Zhao, C. Chen, and B. Shen, "Optimal scheduling of isolated microgrid with an electric vehicle battery swapping station in multi-stakeholder scenarios: A bi-level programming approach via real-time pricing," *Appl. Energy*, vol. 232, pp. 54–68, Dec. 2018, doi: 10.1016/J.APENERGY.2018.09.211.
[23] J. Yan, M. Menghwar, E. Asghar, M. Kumar Panjwani, and Y. Liu, "Real-time energy management for a smart-community microgrid with battery swapping and renewables," *Appl. Energy*, vol. 238, pp. 180–194, Mar. 2019, doi: 10.1016/J.APENERGY.2018.12.078.
[24] A. R. Jordehi, M. S. Javadi, and J. P. S. Catalão, "Energy management in microgrids with battery swap stations and var compensators," *J. Cleaner Prod.*, vol. 272, Nov. 2020, Art. no. 122943, doi: 10.1016/J.JCLEPRO.2020.122943.
[25] C. Li, L. Zhang, Z. Ou, Q. Wang, D. Zhou, and J. Ma, "Robust model of electric vehicle charging station location considering renewable energy and storage equipment," *Energy*, vol. 238, Jan. 2022, Art. no. 121713, doi: 10.1016/J.ENERGY.2021.121713.
[26] S. Deb, K. Tammi, K. Kalita, and P. Mahanta, "Charging station placement for electric vehicles: A case study of guwahati city, India," *IEEE Access*, vol. 7, pp. 100270–100282, 2019, doi: 10.1109/ACCESS.2019.2931055.
[27] M. Z. Zeb, K. Imran, A. Khattak, A. K. Janjua, A. Pal, M. Nadeem, J. Zhang, and S. Khan, "Optimal placement of electric vehicle charging stations in the active distribution network," *IEEE Access*, vol. 8, pp. 68124–68134, 2020, doi: 10.1109/ACCESS.2020.2984127.
[28] S. Deb, X.-Z. Gao, K. Tammi, K. Kalita, and P. Mahanta, "A novel chicken swarm and teaching learning based algorithm for electric vehicle charging station placement problem," *Energy*, vol. 220, Apr. 2021, Art. no. 119645, doi: 10.1016/J.ENERGY.2020.119645.
[29] S. N. Hashemian, M. A. Latify, and G. R. Yousefi, "PEV fast-charging station sizing and placement in coupled transportation-distribution networks considering power line conditioning capability," *IEEE Trans. Smart Grid*, vol. 11, no. 6, pp. 4773–4783, Nov. 2020, doi: 10.1109/TSG.2020.3000113.
[30] A. Awasthi, K. Venkitusamy, S. Padmanaban, R. Selvamuthukumaran, F. Blaabjerg, and A. K. Singh, "Optimal planning of electric vehicle charging station at the distribution system using hybrid optimization algorithm," *Energy*, vol. 133, pp. 70–78, Aug. 2017, doi: 10.1016/J.ENERGY.2017.05.094.
[31] M. J. Mirzaei, A. Kazemi, and O. Homaee, "A probabilistic approach to determine optimal capacity and location of electric vehicles parking lots in distribution networks," *IEEE Trans. Ind. Informat.*, vol. 12, no. 5, pp. 1963–1972, Oct. 2016, doi: 10.1109/TII.2015.2482919.
[32] J. J. Jamian, M. W. Mustafa, H. Mokhlis, and M. A. Baharudin, "Simulation study on optimal placement and sizing of battery switching station units using artificial bee colony algorithm," *Int. J. Electr. Power Energy Syst.*, vol. 55, pp. 592–601, Feb. 2014, doi: 10.1016/J.IJEPES.2013.10.009.
[33] U. Sultana, A. B. Khairuddin, B. Sultana, N. Rasheed, S. H. Qazi, and N. R. Malik, "Placement and sizing of multiple distributed generation and battery swapping stations using grasshopper optimizer algorithm," *Energy*, vol. 165, pp. 408–421, Dec. 2018, doi: 10.1016/J.ENERGY.2018.09.083.
[34] A. Rezaee Jordehi, M. S. Javadi, and J. P. S. Catalão, "Optimal placement of battery swap stations in microgrids with micro pumped hydro storage systems, photovoltaic, wind and geothermal distributed generators," *Int. J. Electr. Power Energy Syst.*, vol. 125, Feb. 2021, Art. no. 106483, doi: 10.1016/J.IJEPES.2020.106483.
[35] C. Viviescas, L. Lima, F. A. Diuana, E. Vasquez, C. Ludovique, G. N. Silva, V. Huback, L. Magalar, A. Szklo, A. F. P. Lucena, R. Schaeffer, and J. R. Paredes, "Contribution of variable renewable energy to increase energy security in Latin America: Complementarity and climate change impacts on wind and solar resources," *Renew. Sustain. Energy Rev.*, vol. 113, Oct. 2019, Art. no. 109232, doi: 10.1016/J.RSER.2019.06.039.
[36] A. Shekhar, V. Prasanth, P. Bauer, and M. Bolech, "Economic viability study of an on-road wireless charging system with a generic driving range estimation method," *Energies*, vol. 9, no. 2, p. 76, Jan. 2016, doi: 10.3390/en9020076.
[37] M. Gallet, T. Massier, and T. Hamacher, "Estimation of the energy demand of electric buses based on real-world data for large-scale public transport networks," *Appl. Energy*, vol. 230, pp. 344–356, Nov. 2018, doi: 10.1016/j.apenergy.2018.08.086.
[38] V. Vita, "Development of a decision-making algorithm for the optimum size and placement of distributed generation units in distribution networks," *Energies*, vol. 10, no. 9, p. 1433, Sep. 2017, doi: 10.3390/EN10091433.
[39] Sileo. *Sileo: E-Bus S18*. Accessed: Aug. 27, 2021. [Online]. Available: https://www.sileo-ebus.com/en/e-bus-models/e-bus-s18/
[40] *China's Nio Lets EV Drivers Swap Batteries in 5 Minutes, Hit the Road*. Accessed: Apr. 2, 2022. [Online]. Available: https://www.caranddriver.com/news/a33670482/nio-swappable-batteries-lease/
[41] *Chinese Electric Vehicle Manufacturer NIO Completed 500 K Times of Battery Swapping*. Accessed: Apr. 2, 2022. [Online]. Available: https://m.energytrend.com/news/view/18065.html

MUSTAFA CAGATAY KOCER received the B.Sc. degree in electrical and electronics engineering from Erciyes University, Kayseri, Turkey, in 2017, and the M.Sc. degree in electrical and computer engineering from Abdullah Gül University, Kayseri, in 2018. He is currently pursuing the Ph.D. degree in electrical engineering and computer science with the Technical University of Berlin, Berlin, Germany. His research interests include the integration of electric vehicles, battery storage systems, and renewables in the power grid and energy markets.

AHMET ONEN (Member, IEEE) received the B.Sc. degree in electrical-electronics engineering from Gaziantep University, in 2005, the M.S. degree in electrical-computer engineering from Clemson University, in 2010, and the Ph.D. degree from the Department of Electrical and Computer Engineering, Virginia Tech, in 2014. He is currently an Associate Professor with Sultan Qaboos University. His research interests include renewable, storage, and EV integration, and artificial intelligence applications in power grids.

JAESUNG JUNG (Member, IEEE) received the B.S. degree in electrical engineering from Chungnam National University, South Korea, the M.S. degree in electrical engineering from North Carolina State University, Raleigh, NC, USA, and the Ph.D. degree in electrical engineering from Virginia Tech, Blacksburg, VA, USA. He is currently a Faculty Member with the Department of Energy Systems Research, Ajou University, South Korea. His research interests include the development and deployment of renewable and sustainable energy technologies.

HAKAN GULTEKIN received the B.S., M.S., and Ph.D. degrees in industrial engineering from Bilkent University, Turkey. He is currently an Associate Professor with the Department of Mechanical and Industrial Engineering, Sultan Qaboos University, Muscat, Oman. His research interests include scheduling, optimization modeling, and exact and heuristic algorithm development, particularly for problems arising in modern manufacturing systems, energy systems, and wireless sensor networks.

SAHIN ALBAYRAK received the Ph.D. degree in computer science and the Habilitation degree from the Technical University of Berlin (TU Berlin), Berlin, Germany, in 1992 and 2002, respectively. He is currently a Professor and the Head of the Chair Agent Technologies in Business Applications and Telecommunication, TU Berlin, where he is also the Founder and the Head of the Distributed Artificial Intelligence Laboratory, employing approximately 120 researchers. He is the Founder of Deutsche Telekom Innovation Laboratories and the German-Turkish Advanced Research Centre for Information and Communication Technology. He is also the founding Director of the Connected Living Association. He serves as an advisor to several government authorities and large-scale companies in both Germany and Turkey. His research interests include next-generation telecommunication services and infrastructure, service-centric architectures, service engineering, autonomous systems, agent-oriented modeling, agent architectures, agent programming languages, mobility-supporting services, supply chain management, smart homes and smart cities, preventive health, and cybersecurity.